Available online at www.sciencedirect.com
ScienceDirect
Journal of the European Ceramic Society 31 (2011) 3033–3043
www.elsevier.com/locate/jeurceramsoc

Transmission electron microscopy on Hf- and Ta-carbides sintered with $TaSi_2$

Laura Silvestroni *, Diletta Sciti

CNR-ISTEC, Institute of Science and Technology for Ceramics, Via Granarolo 64, I-48018 Faenza, Italy

Received 31 January 2011; received in revised form 9 June 2011; accepted 1 July 2011
Available online 28 July 2011

Abstract

The microstructure of hot pressed Hf- and Ta-carbides with 15 vol% of $TaSi_2$ was characterized by X-ray diffraction, scanning and transmission electron microscopy in order to investigate the densification mechanisms.

The microstructure of the carbides was constituted by squared grains and subgrains were recognizable only by transmission electron microscopy: the inner part was constituted by the original MC grain and the outer area by a (M,Ta)C solid solution which grew epitaxially on it. The compositional misfit and the difference of the coefficients of thermal expansion between the two regions were accommodated by 45° grain boundaries and dislocations. At the triple junctions, Ta_5Si_3 and $Ta_{4.8}Si_3C_{0.3}$, with Hf impurities were detected. The grain boundaries were observed to be clean.

The microstructure of the composites containing $TaSi_2$ was subsequently compared to composites sintered with addition of the same amount of $MoSi_2$.

Keywords: Carbides; Transmission electron microscopy; Microstructure; Densification

1. Introduction

Hafnium and tantalum carbide belong to the class of materials known as ultra-high temperature ceramics (UHTCs). These materials are of particular interest because of the unique combination of properties, such as high refractoriness, high electrical conductivity and chemical inertness against molten metals or non-basic slags.[1–3] Applications that take advantage of these properties include refractory linings, electrodes, microelectronics, and cutting tools. Potential applications of these transition metals carbides also include aerospace manufacturing, for example, sharp leading edges of hypersonic atmospheric reentry vehicles, rocket nozzles and scramjet components, where the operating temperatures can exceed 3000 °C.[1–3] The major problems afflicting these carbides are related to a difficult densification capability, a poor oxidation resistance in hypersonic environment and a low fracture toughness (3–5 MPa $m^{1/2}$), which is traduced in a unreliable behavior under severe thermal shock.

In recent years, much effort has been devoted to improve the densification and obtain a fine and homogeneous microstructure of these ultra refractory compounds. Hot pressing at temperatures in the range of 2200–3000 °C is generally required for the densification of monolithic HfC or TaC.[4–9] The temperature needed for densification can be strongly reduced (1400–1800 °C) with small amounts of sintering additives, such as Ni,[10] B_4C and C,[11] $MoSi_2$.[12,13] These additives are believed to favour the elimination of the surface oxides present on the starting powders, which are supposed to hinder the matter transfer among the particles. However, the introduction of secondary phases often leads to grain coarsening, entrapped porosity and poor strength at high temperature.

Previous studies have demonstrated that the addition of silicides of transition metals, such as $MoSi_2$ and $TaSi_2$,[12–16] has positive effects on the densification and high temperature mechanical properties of borides and carbides. In addition, silicides, as silica-forming compounds, can offer significant improvement to the oxidation behavior.

Among the possible additives that can meet the requirements imposed by ultra-high temperature regime, tantalum disilicides is among the most suitable, thanks to its high melting point, 2200 °C, to the formation of a high melting oxide, Ta_2O_5 (1880°)

* Corresponding author. Tel.: +39 0546 699723.
E-mail address: laura.silvestroni@istec.cnr.it (L. Silvestroni).

0955-2219/$ – see front matter © 2011 Elsevier Ltd. All rights reserved.
doi:10.1016/j.jeurceramsoc.2011.07.003

and because Ta can stuff vacancies in Hf-, Zr-oxide and increase the immiscibility of the silica-based external glass, thus retarding the oxygen diffusion inward the bulk.[17] Furthermore, the availability of Si-species which can form a protective silica-based layer is desired upon oxidation.

So far, $TaSi_2$ has been mainly employed in the field of electronics. The use of $TaSi_2$ for UHTCs production is relatively unexplored. Pastor and Meyer[18] studied the effect of addition of $TaSi_2$ and other silicides on the densification and oxidation resistance of ZrB_2, assessing the formation of boride-silicide solid solutions and improvement of oxidation resistance in air up to 1200 °C. Talmy et al.[19] have studied ceramics in the system ZrB_2–Ta_5Si_3 and have reported a significant improvement in the densification, which was fully accomplished at 1900 °C, and of the oxidation resistance in comparison with pure zirconium diboride. Opila et al.[20] studied the influence of $TaSi_2$ addition to ZrB_2–SiC compositions and found a significant improvement in the oxidation resistance at 1627 °C in air. More recently, we studied the microstructure and properties of diborides and carbides processed with $TaSi_2$[16,21].

In this study, the effect of $TaSi_2$ addition on densification and microstructure evolution of HfC and TaC is studied by scanning and transmission electron microscopy.

An overview of the microstructure and the mechanical properties of the compositions under exam is reported in[16] showing that these composites have appealing microstructural features and enhanced mechanical properties compared to the state of the art. Hence, this work aims at updating the microstructural characterization at nanoscale level.

Transmission electron microscopy (TEM) is a powerful tool to explore microstructures on a small length scale to disclose the densification mechanisms. This technique allows acquiring a variety of information with respect to microstructure and composition with high spatial resolution.[22] In order to tailor materials to meet specific requirements such as high temperature performance, the relationship between processing, microstructure, and mechanical behavior has to be known and deeper investigations are mandatory. A thorough literature analysis revealed that very few detailed TEM works on densification mechanisms are available for this class of materials,[14,21,23–25] which however are essential to select the most suitable sintering aid and processing conditions.

2. Experimental procedure

The compositions under investigation are listed in Table 1. The commercial powders utilized for the materials production are reported in Table 2. The powder mixtures were ultrasonically treated in absolute ethanol for 20 min and ball milled for 24 h using zirconia milling media, subsequently dried in a rotary evaporator and sieved to −60 mesh screen size.

Hot pressing was used to densify the $TaSi_2$-contaning composites. The sintering was conducted in low vacuum (∼100 Pa) using an induction-heated graphite die with a constant uniaxial pressure of 30 MPa, heating rate 20 °C/min and free cooling. For each composition, the maximum sintering temperature was set on the basis of the shrinkage curve, as indicated in Table 1.

To identify the crystalline phases formed, all samples were examined using X-ray diffraction (Siemens D500, Karlsruhe, Germany), with CuK_α radiation, step size of 0.04 and 1 s counting rate. In some cases, a Si standard was placed on the sample surface in order to detect eventual peak shift.

The microstructures were analyzed on polished and fractured surfaces by scanning electron microscopy (SEM, Cambridge S360, Cambridge, UK) and energy dispersive X-ray spectroscopy (EDS, INCA Energy 300, Oxford instruments, UK). TEM samples were prepared by cutting 3 mm discs from the bulk of the sintered pellets. These were mechanically ground down to about 20 μm and then further ion beam thinned until small perforation were observed by optical microscope. Local phase analysis was performed using transmission electron microscopy (TEM) equipped with an energy-dispersive X-ray system (FEI, CM12, Eindhoven, The Netherlands; EDS, EDAX Genesis 2000, Ametek GmbH; Wiesbaden, Germany) operating at a nominal voltage of 120 keV. High-resolution investigations were performed using a FEI CM20 STEM operating at a nominal voltage of 200 keV. Quantitative calculations of the microstructural parameters, like residual porosity and secondary phases content, were carried out via image analysis with commercial software package (Image Pro-plus 4.5.1. Media Cybernetics, Silver Springs, MD, USA). Thermodynamic calculations were performed using commercial software HSC Chemistry for Windows 5, (Outokumpu Research Oy, Pori, Finland).

3. Results and discussion

3.1. HfC–$TaSi_2$ composite

According to X-ray diffraction (Fig. 1), no reflections from $TaSi_2$ were detected after sintering. Besides pure HfC (PDF# 39-1491) another phase is clearly visible on the right of the identified peaks, this feature is more evident in the range $2\theta = 85$–$120°$. The unit cell parameter of this newly formed phase is $a = 4.6202$ Å, i.e. shorter than that of pure HfC ($a = 4.6377$ Å), which indicates a contraction of the unit cell. The presence of these additional reflections was interpreted as due to the formation of a (Hf,Ta)C solid solution. On the basis of the Vegard's rule for the HfC–TaC system and hypothesizing that only Ta can enter the HfC structure, it can be estimated that the amount of Ta incorporated into HfC grains was ∼10 at%, giving $(Hf_{0.9}Ta_{0.1})C$ as the composition of the solid solution.

The microstructure of this composite (Fig. 2a and b) is fine and homogenous and the mean grain size of the HfC phase is around 0.8 μm (Table 1), which indicates that no grain coarsening occurred during sintering. By SEM-EDS analysis, tantalum was confirmed to be present in most of the carbide grains (Fig. 2c). Secondary phases in Fig. 2b were less than 5 vol% and included unreacted $TaSi_2$ and Ta–Si-based phases whose stoichiometry was difficult to define, due to the overlapping of the strongest Ta and Si lines. Occasionally, Si–O–C and SiC phases formed large pockets, as shown in Fig. 2d. From the morphology of these areas, it is presumed that a partial or complete carburization of silicon occurred, due to the carbon-rich sintering environment.

Table 1
Composition, sintering parameters, temperature at which the shrinkage started, theoretical and experimental density, mean and maximum grain size of the $TaSi_2$-doped composites.

Sample	Composition (vol%)	Sintering (°C/min)	T_{ON} (°C)	Th. density (g/cm^3)	Exp. density (g/cm^3)	m.g.s. (μm)	Max g.s. (μm)
HCT	HfC–15 $TaSi_2$	1760/10	1600	12.1	12.0	0.8	2.2
TCT	TaC–15 $TaSi_2$	1750/9	1400	13.7	13.3	2.5	5.9

Table 2
Characteristics of the commercial powders utilized for the production of the composites.

Powder	Crystal structure	Supplier	m.g.s. (μm)	Impurities (wt%)
$TaSi_2$	Hexagonal	ABCR, Gmbh & Co. Karlsrhue, Germany	<45	Nb: <10^{-6}
HfC	Cubic	Cerac Inc., Milwaukee, USA	0.80	U: 0.0002 Zr: <0.6 Ca: 0.01 Cd: <0.0007 Cr: <0.0005
TaC	Cubic	Cerac Inc., Milwaukee, USA	0.85	Fe: 0.02 Na: 0.03 Nb: 0.03 Ti: 0.04

By TEM inspection, dislocation activity and subgrain structures were observed in HfC matrix (Fig. 3a), the inner part of the grains was pure HfC and the outer part was a (Hf,Ta)C solid solution, according to EDS analyses. The subgrain morphology, not evidenced by SEM analysis, was revealed by TEM to be constituted by dislocations at the edge between the pure phase and the solid solution. Besides $TaSi_2$ phase, recognizable as a bright phase with irregular shape accommodated among the HfC grains, mixed $(Hf,Ta)_5Si_3$ and $(Hf,Ta)_{4.8}Si_3C_{0.5}$ hexagonal phases were identified by electron diffraction at the triple points with bright contrast (Fig. 3b and c), about 50 nm big. The just mentioned phases without hafnium are well known compounds with the space group $P6_3/mcm$ and with lattice parameters of $a = 7.4700$ and $c = 5.2260$ Å for Ta_5Si_3 and $a = 7.4940$ and $c = 5.2420$ Å for $Ta_{4.8}Si_3C_{0.5}$.[26] These phases derive from the pure tetragonal Ta_5Si_3, which is stabilized to the hexagonal one by carbon impurities. Electron diffraction technique resolution is not precise enough to detect a lattice distortion in Ta_5Si_3 due to Hf substitution, considering that the two metals have very close atomic number. However, a rough estimation of Hf/Ta ratio around 10 at% can be calculated by considering the EDS peaks in the range 7.5–8.5 keV. In contrast, Si amount cannot be quantified due to its strong dependence on the thickness of the specimen.

Some features of the matrix grains, such as Moiré fringes parallel to the operating reflection, dislocations and π-boundaries, are marked in Fig. 3d. The same defective structures were already observed in Si_3N_4 and SiAlONs upon microstructural re-assessment.[27] As previously reported by Hwang et al., these types of dislocation networks and Moiré fringes usually form when there is a rotational misfit between core and shell.[27–29] The formation of the dislocations in the present case could be thus

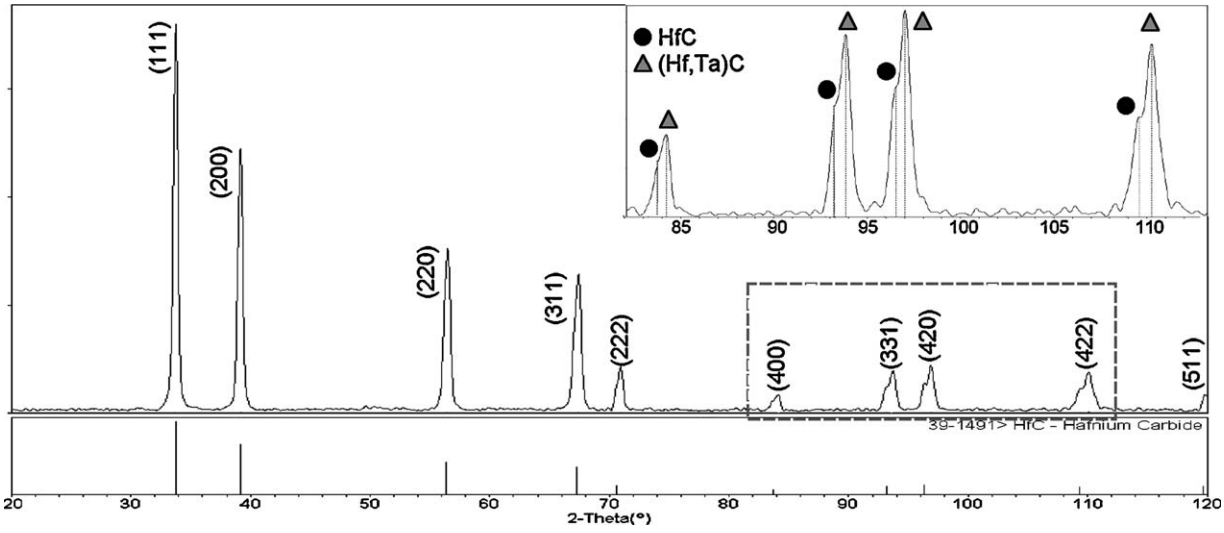

Fig. 1. X-ray diffraction pattern for the HCT composite. In the inset: a magnification of the dotted area; below the spectrum of pure HfC according to PDF# 39-1491.

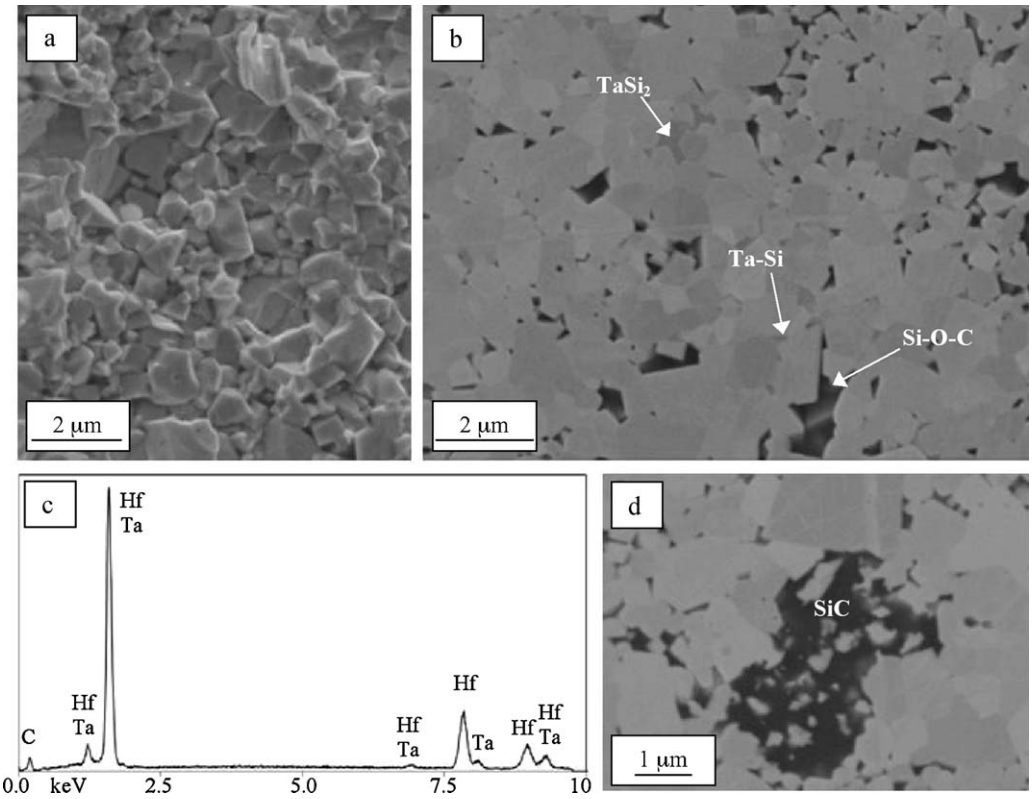

Fig. 2. HfC–$TaSi_2$ composite: (a) fracture and (b) polished sections, (c) typical SEM-EDS spectra collected on HfC grains revealing the presence of Ta, (d) large SiC pocket.

explained by a rotational core/shell misfit, that probably resulted from the different thermal expansion coefficient, in turn related to compositional differences.

High resolution analyses revealed clean grain boundary both at the interface (Hf,Ta)C/$TaSi_2$ and (Hf,Ta)C/(Hf,Ta)C (Fig. 4).

3.2. *TaC–$TaSi_2$ composite*

The X-ray diffraction pattern of this composite is reported in Fig. 5; a Si standard was placed on the top of the specimen in order to detect any peak shift. In the whole 2-Theta range, TaC and $TaSi_2$ were the only crystalline phases detected after sintering. The lattice cell of TaC was found to be smaller 4.4564 Å, than that of the pure phase, 4.4602 Å (PDF#65-0282), which corresponds to a $TaC_{0.98}$ composition. Carbon loss, inducing lattice shrinkage, is very probable in these carbides, owing to the wide stability region of the fcc TaC_x phase.[30] It can also be observed that all the peaks showed asymmetry on the left side, which generally indicates the presence of lattice defects, such as solid solutions. However, different from the HCT composite no clear peak splitting was observed.

The microstructures displayed in Fig. 6 put in evidence little or no residual porosity, Fig. 6a. The micrographs of the polished surface, Fig. 6b, showed that the mean grain size of the carbide phase was 2.5 μm, but coalescence of grains led to the formation of larger grains, up to 6–7 μm. The $TaSi_2$ grains are recognizable as grey phase in a brighter matrix and tended to form large pockets as wide as 3–8 μm (Fig. 6b). Moreover, it can be noticed that $TaSi_2$ phase has very low dihedral angles at the interface with the matrix, showing very ductile behavior. $TaSi_2$ is known to a have a brittle to ductile transition around 1000 °C, similar to $MoSi_2$,[31] thus the high concavity displayed by the silicide could also be due to local liquid phase formation. Dark contrasting features were identified by SEM-EDS as SiC, Si–C–O and SiO_2 (Fig. 6c and d). These dark phases were observed to be adjacent to $TaSi_2$, indicating that they formed consuming $TaSi_2$. According to image analysis, the volumetric amount of $TaSi_2$ in the final microstructure was around 10 vol%, i.e. slightly lower than the initial composition, 15%.

By TEM inspections, 45° grain boundaries were observed in the matrix (Fig. 7a and b). Epitaxy between inner and the external part and the corrugate feature of the sub-grain boundary might indicate lattice misfit. However, the exact stoichiometries of TaC_x phases constituting core and shell could not be assessed, being carbon signal strongly dependent on the specimen thickness. Limiting our speculation to the presence of oxygen peak in the spectrum relative to the outer shell, we can just argue that this phase could be originated from a Ta–Si–C–O liquid phase (Fig. 7a). The possibility to have non stoichiometric TaC_x in the shell is strengthened by the contrasts observed in Fig. 7c, which could be due to vacancies in the lattice. The bright phase surrounded by stress contrast in Fig. 7d is SiC containing low amounts of oxygen. Occasionally, amorphous silica droplets were observed adjacent to SiC grains. At the triple point junctions, Ta_5Si_3 and $Ta_{4.8}Si_3C_{0.3}$ were detected (Fig. 7e). High resolution mode revealed non wetted TaC/TaC interfaces,

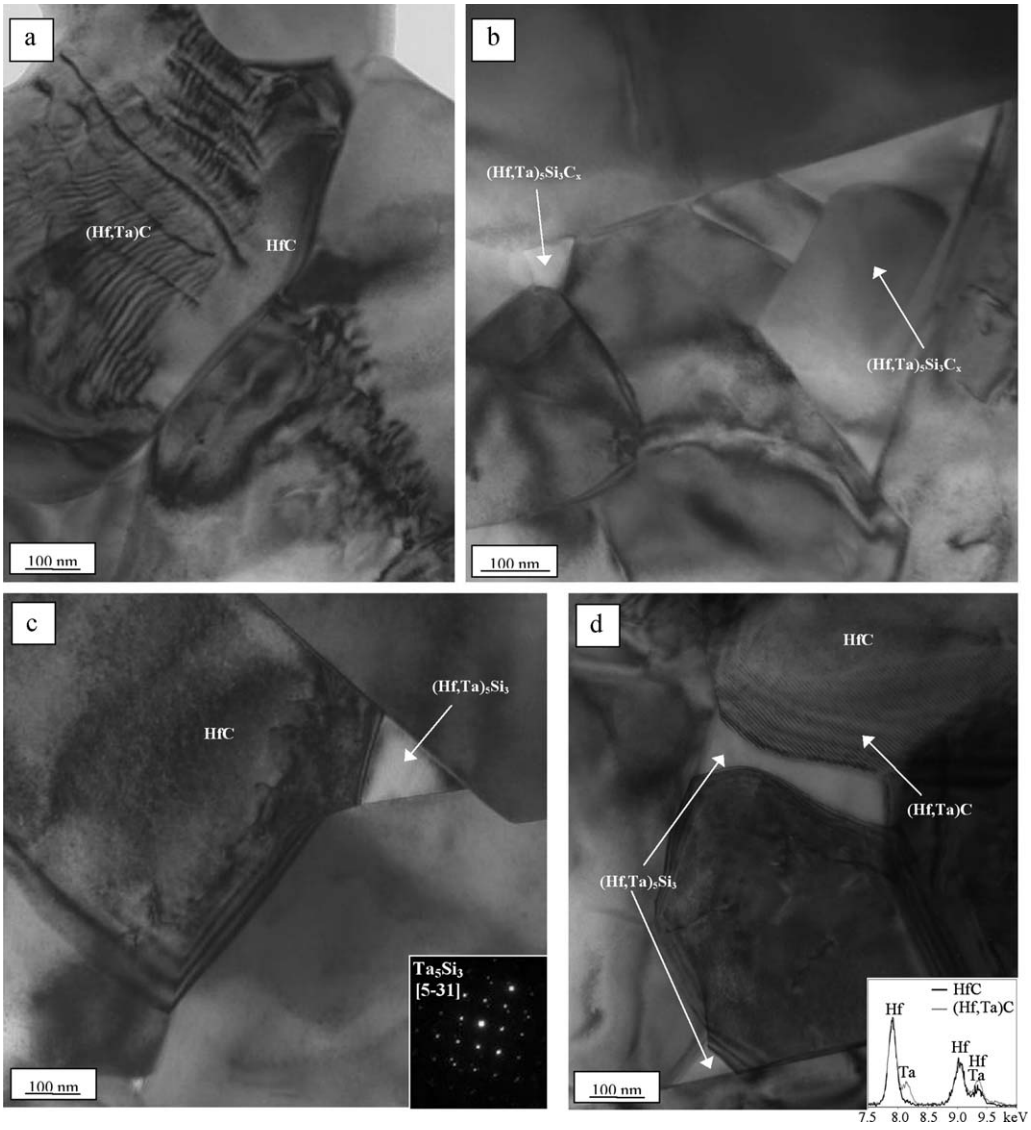

Fig. 3. Bright field TEM images showing (a) dislocation activity between HfC-core and (Hf,Ta)C-shell, (b) an example of agglomerate at the triple point, (c) the Ta_5Si_3 phase with the corresponding diffraction pattern in the inset and (d) an example of microstructure showing the Ta_5Si_3 phase and Moiré fringes in the solid solution. The inset in (d) shows the EDS spectra collected on HfC and (Hf,Ta)C solid solution.

analogously to the previous system; an example is reported in Fig. 7f.

4. Discussion

4.1. Densification mechanism

As far as densification is concerned, different mechanisms are thought to occur for the materials under investigation; however, in order to rebuild the active processes during sintering of the carbides of Hf and Ta with addition of $TaSi_2$, it is useful to summarize the main findings.

- The final microstructure of the two composites is characterized by the formation of Ta-containing solid solutions, which grew epitaxially on the matrix grain. The misfit between the core and the shell was accommodated by corrugated grain boundaries. These features suggest a solubility of Ta in HfC and confirm the wide range of fcc TaC_x stability.
- Investigations of the triple points revealed the formation of further silicides, such as Ta_5Si_3 or $Ta_{4.8}Si_3C_{0.3}$, which contained Hf impurities. This aspect reveals a mutual solubility of Hf in Ta–Si-based phases.
- High resolution TEM evidenced clean grain boundaries in the carbide matrix.

Several aspects of the densification process will be taken in exam to figure out the path sequence leading to the final microstructure.

4.1.1. Reactive environment

Let's first investigate the possible origin of the volatile species developed in the early stage of sintering.

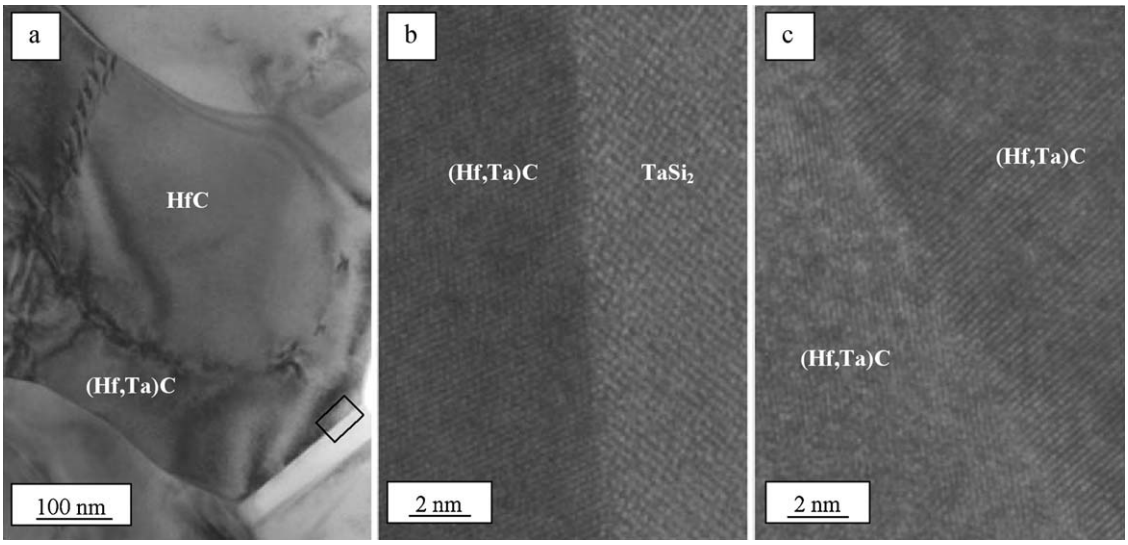

Fig. 4. BF-TEM images evidencing (a) dislocations pile-up between HfC and (Hf,Ta)C, (b) clean grain boundary of the squared box in (a) between the solid solution and $TaSi_2$ and between two adjacent solid solution grains in (c).

During hot pressing, the pressure increased in the vacuum chamber between 1200 and 1600 °C, due to development of gaseous species after interaction of $TaSi_2$ with CO generated inside the graphite-rich environment of the furnace. Sources of carbon are easy to identify in the compositions investigated. Carbides are C donors and further contamination may occur during sintering, which is conducted in a graphite-rich environment (die and rams).

Using a commercial software package (HSC Chemistry for Windows 5, Outokumpu Research Oy, Pori, Finland), some potential reactions between $TaSi_2$ and CO were analyzed in the range 1200–1900 °C under a pressure of 100 Pa, i.e. approximately the vacuum level inside the hot-press chamber, considering pure phases with the activity equal to one. For simplicity, the molar ratio between the phases was taken equal to one. Molar products resulting from $TaSi_2$ + CO are displayed in Fig. 8.

According to this thermodynamic analysis, it can be read that: CO promotes $TaSi_2$ decomposition with the formation of SiO gas at $T \geq 1200$ °C and Si(g) at $T \geq 1600$ °C. The formation

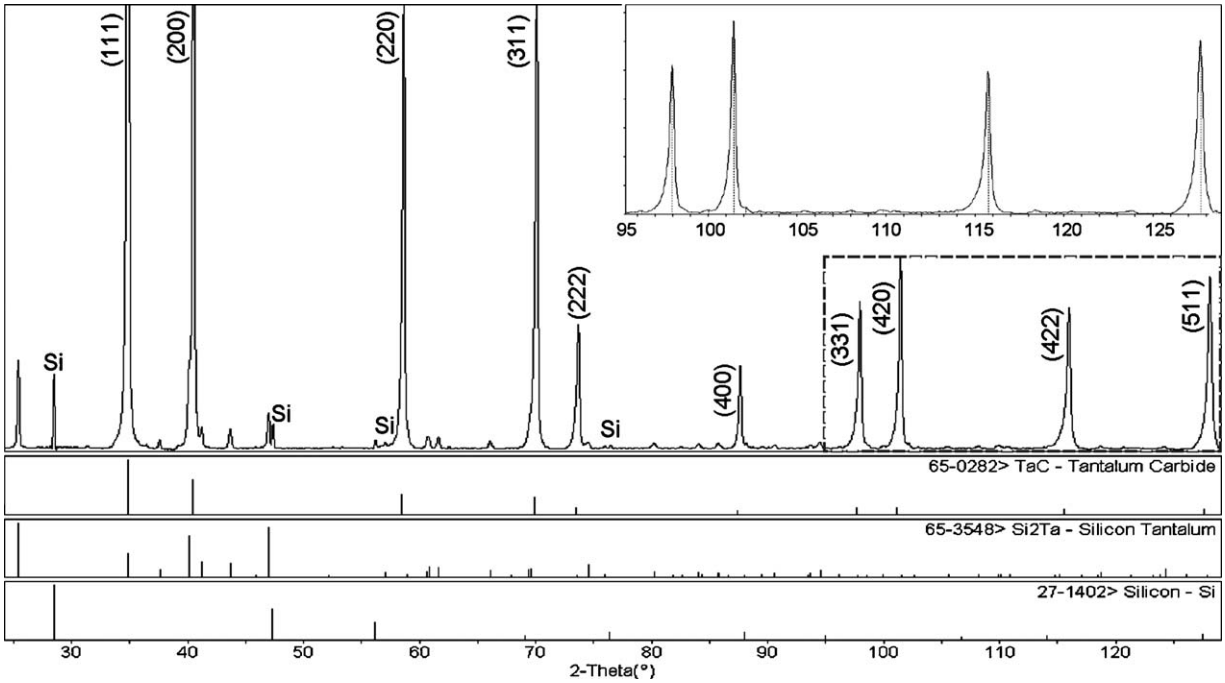

Fig. 5. X-ray diffraction pattern for the TCT composite carried out with a Si standard: indexes refer to TaC phase, minor peaks refer to $TaSi_2$. In the inset: a magnification of the dotted area showing peaks asymmetry; below the peaks position of pure TaC, $TaSi_2$ and Si according to the PDF files.

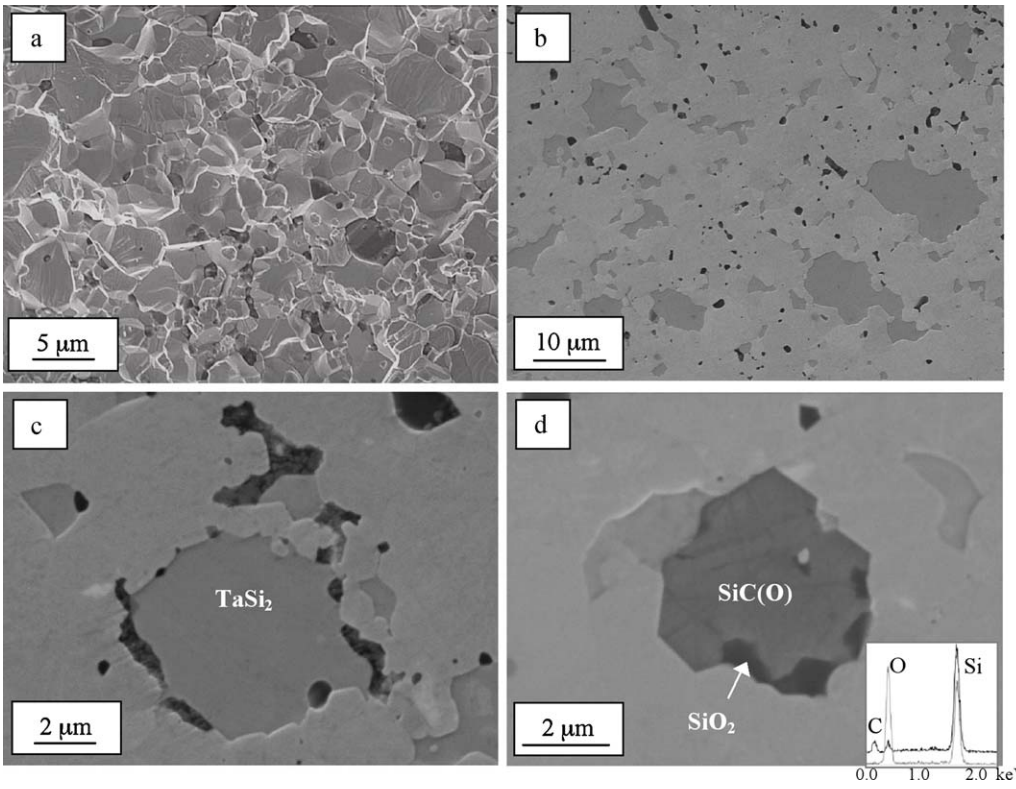

Fig. 6. SEM images of the TaC–$TaSi_2$ composite: (a) fracture and (b, d) polished sections. The inset in (d) shows the EDS spectra of Si–O–C and SiO_2.

of TaC is expected above 1200 °C, whilst the formation of SiC seems to become unfavorable with increasing temperature. In the range 1450–1850 °C, the formation of liquid Si is predicted. The change in the Gibbs free energy varies from -0.9×10^3 kJ at 1200 °C to -1.3×10^3 kJ at 1900 °C.

The above thermodynamic predictions are in partial agreement with the microstructural observations and suggest that C and/or CO play a key role in the chemistry of these systems. $TaSi_2$ decomposition and consequent SiO volatilization was confirmed by the pressure increase in the furnace chamber and microstructural analyses which revealed lower amounts of $TaSi_2$ compared to the initial content for the two composites.

From these analyses it can be concluded that the most important reaction occurring during sintering of the $TaSi_2$-containing composites is:

$$TaSi_2 + CO(g) = TaC + 2Si(l) + SiO(g) \quad (1)$$

Since carbides are C donor and sintering is conducted in a C-rich furnace, carbon is the dominant moving species, so we can hypothesize the following reaction to occur:

$$Si(l) + C = SiC \quad (2)$$

The newly formed TaC from reaction (1) can enter in solid solution with HfC, according to:

$$TaC + HfC = (Hf, Ta)C \quad (3)$$

The reduction of $TaSi_2$ content after sintering confirms the tendency to decomposition of this silicide in reducing atmosphere. The formation of liquid silicon at relatively low temperature (reaction (1)) is compatible with the enhanced sintering activity of the HfC-$TaSi_2$ compositions, with respect to other HfC-based ones. SiC phases deriving from carburization of silicon (reaction (2)) are present in the microstructure of both composites (Figs. 2d and 6d). For the HCT composite, the formation of TaC was not observed, but occurrence of reaction (3) was verified by microstructural analyses and X-ray diffraction. Indeed, it is well known that the solubility between carbides of Group IV and monocarbides of Group V is complete and they are expected to form solid solutions.[32] In the TCT composite, TaC formation from reaction (1) is more difficult to track, as, with the EDS technique, it is tricky to detect the difference in stoichiometry between TaC-core and TaC-shell. However, also for this composite, Si-based phases are present in the microstructure and the final content of $TaSi_2$ is nearly halved as compared to the starting composition.

4.1.2. Liquid phase formation

From the previous paragraph, the main implication is that sintering is assisted by liquid phase. This hypothesis is further strengthened by irregular shape displayed by the $TaSi_2$ phase, as well as by the microstructural coarsening of the composites, as indicated in Table 3.

One evidence of the formation of liquid silicon, formed after reaction (1), is the temperature at which TCT composite started to shrink (T_{ON} in Table 1), which occurred indeed at 1400 °C. In addition, others can be the sources of liquid that will be examined in relation to the available phase diagrams.

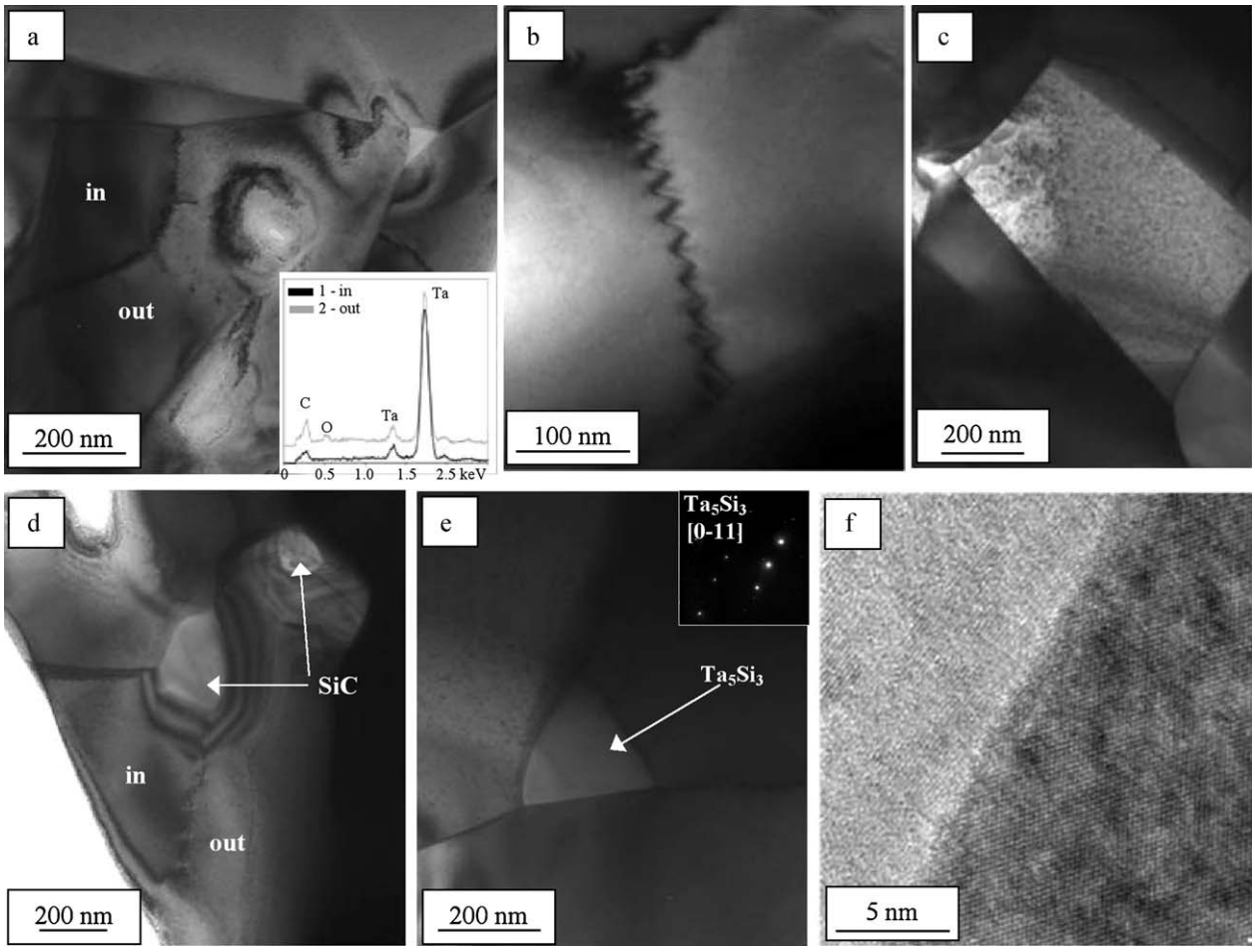

Fig. 7. TEM images showing (a, b) the interface between TaC-in and TaC-out with the corresponding EDS spectra in the inset; (c) contrasts in a TaC grain suggesting vacancies, (d) crystalline SiC among TaC matrix, (e) Ta_5Si_3 at the triple point and (f) high resolution image showing a clean boundary at the TaC/TaC interface.

In the Ta–Si phase diagram,[33] $TaSi_2$ and Ta_5Si_3 form a eutectic at 1970 °C, but this temperature exceeds the sintering ones (1750–1760 °C), so it can be discarded.

Subsequently, in the temperatures range 1690–1700 °C another eutectic is predicted between the HfO_2 and SiO_2, which cover the starting particles.[34] Since Hf traces were detected in SiO_2 pockets by TEM-EDS, also this liquid cannot be ruled out. The corresponding Ta_2O_5–SiO_2 phase diagram foresees a eutectic at 1887 °C,[35] but this temperature is out of the sintering temperature range (1750–1760 °C).

Besides these pseudo-binary systems, Ta–Si–C ternary system is also relevant.[26,36] Unfortunately, the position of the liquidus surfaces is not indicated, as only the isothermal section is available to indicate the phases at equilibrium with one another. In addition, the same system including oxygen is not accessible in the literature.

Hence we can just deduce from microstructural features what was the composition of the liquid phase. The crystallized triple points were Ta_5Si_3 and $Ta_{4.8}Si_3C_{0.3}$ with Hf impurities. Moreover in the solid solution region, oxygen traces were detected, that means this liquid dragged oxygen-bearing species present on the particles surface.

It can be therefore concluded that a Ta–Si–C–O based liquid, where Hf (and Ta) were soluble in, formed during densification.

Table 3
Comparison of the mean (m.g.s.) and Max (M.g.s.) grain sizes between hot pressed ceramics with addition of 15 vol% of $TaSi_2$ or $MoSi_2$.[16] Δ% is referred to the starting powder dimensions. The sintering cycles are reported too in order to underline the grain coarsening. For all the composites the same pressure was applied. σ_{RT}, σ_{1200}: 4-pt flexural strength at room temperature and at 1200 °C in Ar flux. $\Delta\sigma$: strength decrease from room temperature to 1200 °C.

Sample	Composition (vol%)	Sintering (°C, min)	Matrix start. powder (μm)	m.g.s. (μm)	Δm.g.s. (%)	M.g.s. (μm)	ΔM.g.s. (%)	σ_{RT} (MPa)	σ_{1200} (MPa)	$\Delta\sigma$ (%)
HCT	HfC + 15$TaSi_2$	1760/10	0.8	0.8	0	2.2	175	464 ± 95	394 ± 27	15
HCM	HfC + 15$MoSi_2$	1900/10	0.8	1.2	50	2.3	188	417 ± 38	294 ± 39	29
TCT	TaC + 15$TaSi_2$	1750/9	0.9	2.5	194	5.9	594	679 ± 18	429 ± 35	37
TCM	TaC + 15$MoSi_2$	1850/3	0.9	1.2	41	3.7	335	900 ± 33	537 ± 45	40

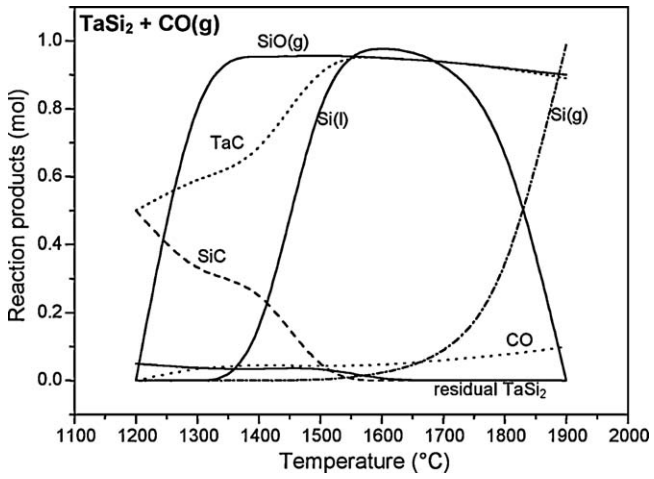

Fig. 8. Molar content of the products deriving from the reactions 1 mol $TaSi_2$ + 1 mol CO(g), as a function of the temperature at constant pressure of 100 Pa.

4.1.3. Formation of solid solutions

The nature of bonding in the carbides is known to be a mixture of covalent and metallic bonding with little ionic tendency. If solid solutions were formed, Ta from $TaSi_2$ substituted the transition metal atoms in the carbide lattice. This may occur either by cations diffusion or by solution-precipitation. Given the low diffusion coefficient of this class of materials, it is presumed that lattice diffusion can occur only at very high temperature. Indeed, solution re-precipitation seems to be the dominant mechanism, in light of the sintering behavior characterized by a relatively low T_{ON}, 1400–1600 °C (Table 2). The well defined boundary between core and shell also puts forward a re-precipitation from liquid phase over a diffusion process.

The mechanism which led to the formation of final microstructure is sketched in Fig. 9 and can be summarized as follows. The MC grains were initially surrounded by $TaSi_2$, which was ductile at temperature above 1000 °C. At temperature above 1200 °C and in presence of CO, $TaSi_2$ started to decompose into Ta and Si/SiO/SiO_2 forming a liquid phase where the carbides partially dissolved in. When the solubility limit was reached, M–C precipitated on the original MC seed dragging Ta and O from the liquid phase. At the same time, crystalline Ta–Si–C phases precipitated from the liquid and were confined to the triple junctions, leaving clean boundaries.

Because of the compositional differences and the coefficients of thermal expansion misfit between the original MC core and the Ta-containing MC shell, dislocation networks formed in the region of non coherency, i.e. at the grain boundary between core and shell, as illustrated for example in Figs. 4a and 7a, b.

Keeping in mind the mean grain size of HfC and TaC starting powder, both around 0.8 μm, it can be noticed that the final mean grain size of the composites was markedly different, despite very similar sintering temperatures (Table 1). The coarsest grains in HCT were 2.2 μm, whilst 5.9 μm in TCT. This feature can be related to the nature of the guest cation. We can expect indeed that Ta from $TaSi_2$ is more easily hosted by TaC than by HfC.

4.2. Comparison with UHTCs containing $MoSi_2$

In this section the microstructures above presented will be compared to the microstructures of previously analyzed materials containing $MoSi_2$ as sintering additive.[16] Table 3 summarizes the most important densification and microstructural features of the composites.

The decomposition of $TaSi_2$ and formation of liquid Si at relatively low temperatures can be considered the key event inducing the earlier densification of $TaSi_2$-containing composites compared to $MoSi_2$-containing ones (1750 °C vs 1850–1900 °C for $MoSi_2$ additions). The reducing environment strongly favors $TaSi_2$ decomposition, which is traduced in quicker formation of liquid phase and in lower sintering temperatures.

For both sintering additives, the presence of Mo/Ta-silicocarbides with the 5:3 stoichiometry was observed at the triple points containing Hf impurities. It seems proved that this phase has a higher tendency to host interstitial cations, more than the

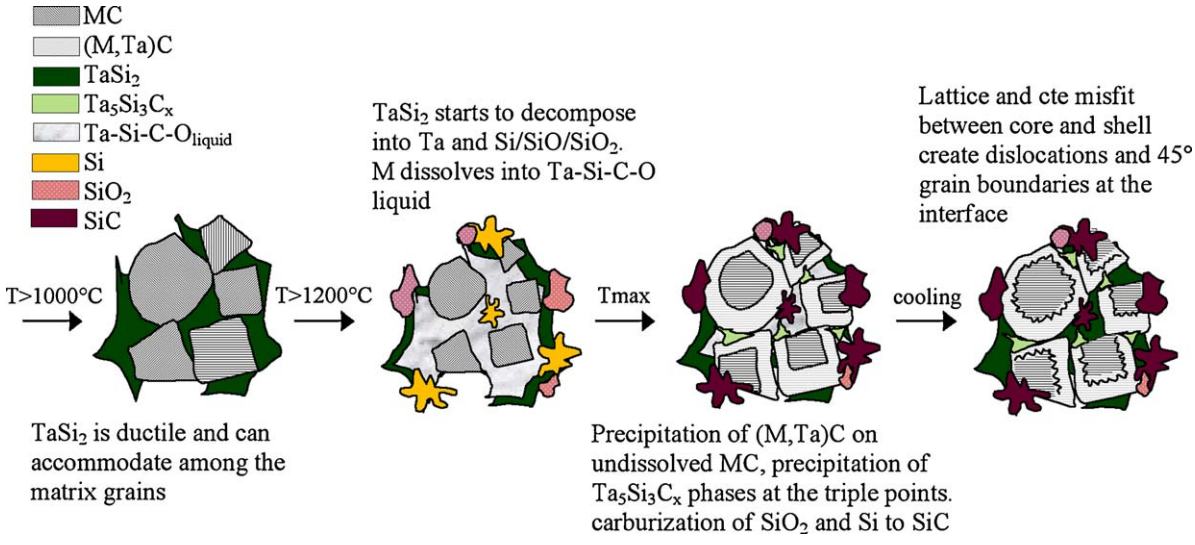

Fig. 9. Sketch of the possible densification mechanisms occurring during sintering of HfC and TaC with $TaSi_2$.

silicides with 1:2 stoichiometry. To note that, these 5:3 silicides generally have higher melting points and lower creep rate than the 1:2,[37] hence the formation of these refractory phases at the triple points can be beneficial for high temperature properties, as they can pin the microstructure and hinder the sliding of the grain boundaries, increasing the structural resistance of these ceramics.

The liquid phase at the sintering temperature was presumably constituted by Mo/Ta–Si–C–O, and non-wetted interfaces were found when either $MoSi_2$ or $TaSi_2$ were added to either HfC or TaC. It can be hypothesized that the liquid formed in the carbides at around 1400 °C had high viscosity and tended not to completely flow through the grains leaving clean grain boundaries. On the contrary, borides of Zr and Hf sintered with addition of $MoSi_2$[23] or $TaSi_2$[21] displayed wetted interfaces, owing to the presence of boron in the liquid phase, which lowered the viscosity.[38]

Finally, another striking difference is the formation of dislocations at the core-shell interface in the $TaSi_2$-doped composites that has never been observed in $MoSi_2$-doped ones. This can be explained in terms of higher content of Ta in the solid solution, i.e. ∼10 at% in HCT. As a matter of fact, (Mo,M)C was barely detected in a ZrC–$MoSi_2$ composite,[14] confirming a negligible solid solubility of Mo in transition metals carbides. On the contrary, (Ta,M)C were confirmed by XRD, SEM and TEM analysis. The higher content of Ta in the solid solution led to a more pronounced difference of lattice parameters and coefficients of thermal expansion between core and shell, resulting in 45° grain boundaries and dislocations.

A direct consequence of the presence of dislocations and sub-grains is the enhancement of impurity or cations diffusion through the dislocation core, which might continue to happen even in the last stage of sintering. Diffusion through these discontinuous paths is 10^6 times faster than in the bulk.[39] This phenomenon might have enhanced the mass transfer as well and hence the densification of $TaSi_2$-containing ceramics over $MoSi_2$-containing materials.

5. Conclusions

The microstructure of hot pressed Hf and Ta carbides with addition of 15 vol% $TaSi_2$ was studied through X-ray diffraction, scanning and transmission electron microscopy.

$TaSi_2$ played an essential role in the densification through different mechanisms. In reducing environment (C/CO-rich), $TaSi_2$ partially dissociated into Ta and Si/SiO/SiO_2 phases, which favoured the formation of liquid phases where the matrices were partially soluble in. The liquid was constituted by Ta–Si–C–O and, upon cooling, it crystallized at the triple points in form of Ta_5Si_3 and $Ta_{4.8}Si_3C_{0.5}$, leaving clean grain boundaries. Traces of oxygen in the phases at the triple junctions confirmed that the liquid was effective in removing the oxide layer covering the starting powders, which is well known to hinder the densification of non-oxide ceramics.

All the composites presented a core/shell morphology type, where the core was constituted by the original grain, MC, and the shell was a (M,Ta)C solid solution. At the core/shell interface 45° grain boundaries or dislocations were observed and, generally, many lattice defects were present in the solid solution. The internal corrugate sub-boundary presumably formed to accommodate the lattice mismatch and the different coefficients of thermal expansion between the original core and the Ta-containing shell. The core/shell had the same orientation, suggesting that epitaxial growth started from the undissolved matrix and then eventually resulted in the core/shell structure.

Compared to $MoSi_2$, $TaSi_2$ showed to be more effective in enhancing the densification, thanks to its capability to form liquid phases at lower temperature and its higher mutual solubility towards the matrices.

Therefore, $TaSi_2$ performed multiple beneficial functions on transition metal carbides:

- it allowed the densification of HfC and TaC at lower temperature than conventional (1750 vs 2000 °C),
- it formed higher melting point compounds, 5:3 Ta-silicides, which are very probably helpful for the high temperature properties,
- it provided silica, which is useful to improve the oxidation resistance of the bulk.

Acknowledgements

One of the authors, L.S., wishes to express her gratitude to the AFOSR, in particular the contract monitor Dr. Joan Fuller, for providing support for this project, through the research grant FA8655-09-M-4002. Dr. G. Celotti (CNR-ISTEC, Italy) is acknowledged for the fruitful discussions on X-ray diffraction spectra and Prof. H.J. Kleebe's group (Technische Universität Darmstadt, Germany) is greatly acknowledged for technical assistance during TEM analyses.

References

1. Toth LE. Transition metal carbides and nitrides. In: Margrave JL, editor. *Refractory materials, a series of monographs*. New York: Academic Press Inc.; 1971. p. 6–10.
2. Storms EK. The refractory carbides. In: Margrave JL, editor. *Refractory materials, a series of monographs*. New York: Academic Press Inc.; 1967. p. 94.
3. Shvab SA, Egorov FF. Structure and some properties of sintered tantalum carbide. *Sov Powder Metall Metal Ceram* 1982;**21**:894–7.
4. Opeka MM, Talmy IG, Wuchina EJ, Zaykoski JA, Causey SJ. Mechanical, thermal, and oxidation properties of refractory hafnium and zirconium compounds. *J Eur Ceram Soc* 1999;**19**:2405–14.
5. Wuchina EJ, Opeka MM, Causey SJ, Buesking K, Spain J, Cull A, et al. Designing for ultrahigh-temperature applications: the mechanical and thermal properties of HfB_2, HfCx, HfNx and αHf(N). *J Mater Sci* 2004;**39**:5939–49.
6. Chamberlain AL, Fahrenholtz WG, Hilmas GE, Ellerby DT. High strength ZrB_2-based ceramics. *J Am Ceram Soc* 2004;**87**:1170–2.
7. Samonov GV, Petrikina RY. Sintering of metals, carbides, and oxides by hot pressing. *Phys Sintering* 1970;**2**:1–20.
8. Jackson JS. Hot pressing high-temperature compounds. *Powder Metall* 1961;**8**:73–100.
9. Ramqvist L. Hot pressing of metallic carbides. *Powder Metall* 1966;**9**:26–46.

10. Roeder E, Klerk M. Studies with the electron-beam microanalyzer on hot-pressed tantalum carbide having small additions of manganese and nickel. *Z Metallkd* 1963;**54**:462–70.
11. Zhang X, Hilmas GE, Fahrenholtz WG, Deason DM. Hot pressing of tantalum carbide with and without sintering additives. *J Am Ceram Soc* 2007;**90**:393–401.
12. Sciti D, Sivestroni L, Bellosi A. High density pressureless sintered HfC-based composites. *J Am Ceram Soc* 2006;**89**:2668–70.
13. Silvestroni L, Bellosi A, Melandri C, Sciti D, Liu JX, Zhang GJ. Microstructure and properties of HfC and TaC-based ceramics obtained by ultrafine powder. *J Eur Ceram Soc* 2011;**31**:619–27.
14. Silvestroni L, Sciti D, Kling J, Lauterbach S, Kleebe HJ. Sintering mechanisms of zirconium and hafnium carbides doped with $MoSi_2$. *J Am Ceram Soc* 2009;**92**:1574–9.
15. Silvestroni L, Sciti D. Reactivity, microstructure and mechanical properties of pressureless sintered ultra-refractory carbides. *Adv Mater Sci Eng*, in press, doi:10.1155/2010/835018.
16. Sciti D, Silvestroni L, Guicciardi S, Dalle Fabbriche D, Bellosi A. Processing, mechanical properties and oxidation behavior of TaC and HfC composites containing 15 vol% $TaSi_2$ or $MoSi_2$. *J Mater Res* 2009;**24**:2056–65.
17. Levine SR, Opila EJ. Tantalum addition to zirconium diboride for improved oxidation resistance. NASA/TM-2003-212483, July 2003.
18. Pastor H, Meyer R. An investigation of the effect of additions of metal silicides on titanium and zirconium borides from the point of view of their sintering behavior and their resistance to oxidation at high temperature. *Rev Int Htes Temp Refract* 1974;**2**:41–54.
19. Talmy IG, Zaykoski JA, Opeka MM, Smith AH. Properties of ceramics in the system ZrB_2–Ta_5Si_3. *J Mater Res* 2006;**21**:2593–9.
20. Opila E, Levine S, Lorincz J. Oxidation of ZrB_2 and HfB_2-based ultra-high temperature ceramics: effect of Ta additions. *J Mater Sci* 2004;**39**:5969–77.
21. Silvestroni L, Sciti D. Densification of ZrB_2–$TaSi_2$ and HfB_2–$TaSi_2$ ultra-high-temperature ceramic composites. *J Am Ceram Soc* 2011;**94**:1920–30.
22. Kleebe HJ, Braue W, Schmidt H, Pezzotti G, Ziegler G. Transmission electron microscopy in ceramic materials. *J Eur Ceram Soc* 1996;**16**:339–51.
23. Silvestroni L, Sciti D, Kleebe HJ, Lauterbach S, Müller M. Transmission electron microscopy on Zr- and Hf-borides doped with $MoSi_2$: densification mechanisms. *J Mater Res* 2010;**25**:828–34.
24. Biswas K, Basu B, Suri AK, Chattopadhyay K. A TEM study on TiB_2–20%$MoSi_2$ composite: microstructure development and densification mechanism. *Scr Mater* 2006;**54**:1363–8.
25. Zou J, Sun SK, Zhang GJ, Kan YM, Wang PL, Ohji T. Chemical reactions anisotropic grain growth and sintering mechanisms of self-reinforced ZrB_2–SiC doped with WC. *J Am Ceram Soc* 2011;**94**:1575–83.
26. Gusev AI. Phase equilibria in M–X–X' and M–Al–X ternary systems (M = transition metal; X,X' = B,C,N, Si) and the crystal chemistry of ternary compounds. *Russ Chem Rev* 1996;**65**:379–419.
27. Hwang SL, Chen IW. Nucleation and growth of β′-SiAlON. *J Am Ceram Soc* 1994;**77**:1719–28.
28. Lu HH, Huang JL. Microstructure in silicon nitride containing β-phase seeding: III, grain growth and coalescence. *J Am Ceram Soc* 2001;**84**:1891–5.
29. Lee WE, Hilmas GE. Microstructural changes in β-Si_3N_4 grains upon crystallizing the grain boundary glass. *J Am Ceram Soc* 1989;**72**:1931–7.
30. Santoro G. Variation of some properties of tantalum carbide with carbon content. *Trans Metal Soc AIME* 1963;**227**:1361–8.
31. Simner SP, Xiao P, Derby B. Processing and microstructural characterization of RBSiC–$TaSi_2$ composites. *J Mater Sci* 1998;**33**:5557–68.
32. Pierson HO. *Handbook of refractory carbides and nitrides*. William Andrew Publishing/Noyes Westwood; 1996, 68 pp.
33. Schlesinger ME. The Si–Ta system. *J Phase Equilib* 1994;**15**:90–5.
34. Parfenkov UN, Grebenshchikov RG, Toropov NA. Phase equilibrius in the hafniumdioxide-silicon dioxide system. *Dokl Akad Nauk SSSR* 1969;**185**:840–2.
35. Roth RS, Waring JL. Phase diagrams for ceramists 1970; Diagram 4448.
36. Schuster JC. Investigations in the ternary systems V–Si–C and Ta–Si–C. *J Chim Phys* 1993;**90**:373–8.
37. Chu F, Thoma DJ, McClellan K, Peralta P, He Y. Synthesis and properties of Mo_5Si_3 single crystals. *Intermet* 1999;**7**:611–20.
38. Karlsdottir SN, Halloran JW, Henderson CE. Convection patterns in liquid oxide films on Zr_{B2}–SiC composites oxidized at a high temperature. *J Am Ceram Soc* 2007;**90**:2863–7.
39. Nöllmann I, Trigubo AB. Walsöe de Reca NE, Subgrain structure and dislocation density in annealed MCT. *Jpn J Appl Phys* 1991;**30**:1787–91.